The Debye temperature of iron nanoparticles : how far from the bulk ?

T. Vasina, J. Bernard, Magali Benoit, F. Calvo

The Debye temperature of iron nanoparticles: how far from the bulk?

T. Vasina and F. Calvo
Univ. Grenoble Alpes, LIPHY, F-38000 Grenoble, France and CNRS, LIPHY, F-38000 Grenoble, France

J. Bernard and M. Benoit
CEMES-CNRS, 29 rue Jeanne Marvig, 31055 Toulouse Cedex, France

(Dated: March 4, 2022)

The Debye temperature Θ_D characterizes the vibrations of a solid and marks the transition between quantized and classical behaviors of nuclear motion. While thermodynamical theories suggest that for nanoparticles Θ_D should be lower than the bulk limit and increase with increasing nanoparticle size, various experimental measurements have reported intriguing variations with size, including values above the bulk limit and possibly decreasing with size. In this article we have theoretically determined the Debye temperature of iron nanoparticles of up to about 7 nm diameter at the atomistic level of details, using complementary approaches based on the equilibrium heat capacity or the mean square atomic displacement. Both methods consistently indicate steady finite size effects in the scaling regime, with no evidence for values higher than the bulk or varying in opposite ways, but they also produce marked quantitative differences. Further comparison with the melting temperature T_m indicates that the two quantities correlate with each other through $T_m \propto \Theta_D^\alpha$, but with an exponent α close to 3 that deviates from the expected value of classical thermodynamical theories based on pure bulk ingredients.

I. INTRODUCTION

The vibrations in nanoparticles differ mostly from those in a bulk material owing to the presence of their free surface. This can be exploited to tune their acoustic response,[1] which in turn is of potential interest for practical applications involving their manipulation,[2] mechanical stability[3] to heat transport.[4] One fundamental property that is particularly sensitive to the vibrations of a solid is the Debye temperature Θ_D, which describes its low temperature specific heat as if the system was assumed to behave accordingly with the Debye model of lattice vibrations. In bulk materials, the Debye model reproduces fairly well the phonons contribution to the specific heat, in particular at low (T^3 behavior) and high (Dulong-Petit limit) temperatures. The Debye temperature can thus be considered as a limiting value between the quantum mechanical and classical regimes of vibrations in the solid.

Over the past decades, various experimental efforts have been dedicated to measuring the Debye temperature in low-dimensional systems and in particular metallic nanoparticles, including gold[5–7], platinum[8,9], cobalt[10] iron[11,12], as well as bimetallic systems.[13] From these investigations, quite diverse conclusions were reached regarding how the Debye temperature varies with increasing nanoparticle size N. In most cases, $\Theta_D(N)$ exhibits values lower than the bulk limit Θ_D^∞, and tends to increase with increasing nanoparticle size. This behavior was notably found for Debye temperatures inferred from Raman[6,7] or Mössbauer[10,11] spectroscopy measurements. Such monotonic corrections to the bulk limit are expected based on thermodynamical arguments, in particular those relying on the connection with the Lindemann theory of melting that assumes specific scaling relations with the cohesive energy or the melting temperature,[14] combined with other semiempirical law describing the size variations of the melting temperature itself.[15] Such phenomenological approaches using classical ingredients temperature have been used by other groups in the past at the nanoscale.[16,17] For isolated nanoparticles, they necessarily predict a depression in the Debye temperature, with a magnitude that scales approximately linearly with inverse particle radius. Similar scalings are also expected for other characteristic frequencies of the material, such as the breathing frequency that is accessible through Raman or pump-probe spectroscopic measurements.[18,19]

However, other measurements relying on x-ray techniques have suggested deviations to the bulk behavior that are in striking contrast with thermodynamical predictions, in particular for platinum where a non-monotonic dependence of Θ_D with increasing size was reported,[8,9] with values higher than the bulk. For iron, a decrease with increasing particle size was found by Cuenya and coworkers,[12] the values residing this time below than the bulk limit. Such results are all the more surprising that they are often associated with other equally unusual phenomena such as lower-than-bulk[20] or even negative[8,21] thermal expansion coefficients. While these results are difficult to reconcile with classical thermodynamical theories without invoking arguments related to the environment of the nanoparticles, a critical discussion of such measurements based on x-ray profile analyses (extended x-ray absorption fine structure or near-resonant inelastic x-ray scattering) recently concluded that non-bulk behavior could also be an interpretation artifact of these techniques.[22]

Another contribution to this confusion probably originates from that various quantities have been employed to determine Θ_D depending on the nature of the ex-

periment. This issue is also well known in bulk materials, where different values of Θ_D, possibly carrying some dependence on the measurement temperature itself, are available. For nanoparticles, the standard approach relies on the determination of heat capacities from vibrational densities of states, either obtained from x-ray or Raman techniques. Alternatively, in Mössbauer spectroscopy Θ_D is inferred from the mean square atomic displacement σ^2 through the Debye-Waller factor. Furthermore, Θ_D can also carry some dependence on experimental temperature T_{exp} if the specific value of the heat capacity C_v (or σ^2) at this temperature is assigned to the Debye model, rather than fitting entire temperature-dependent curves $C_v(T)$ or $\sigma^2(T)$ obtained over a broad range of temperatures. The use of macroscopic models to describe finite size systems is also always possibly problematic, and this is obviously particularly true for the smallest clusters containing 10 to 100 atoms approximately.[23–25] In the case of the Debye temperature, the discrete vibrational spectrum necessarily conveys to variations of the heat capacity at low temperature that are exponentially increasing, rather than the expected T^3 behavior in bulk solids.[24] The parameter causing this exponential character is the lowest vibrational frequency in the system, also sometimes called acoustic gap, which is expected to decrease with increasing nanoparticle size.[19] However, even considering that the Debye model for lattice vibrations can be applied phenomenologically to finite systems, it remains unclear why the thermodynamic approach relating the melting temperature to the square of the Debye temperature in a linear fashion, as suggested by Yang and coworkers,[14,15] should also hold for nanoparticles.

To clarify all these issues, we have conducted a detailed computational investigation of the Debye temperature of iron nanoparticles described at the atomistic level of details, comparing various approaches together and against available thermodynamical theories but without assuming them to hold in the first place. The choice of iron is motivated by the availability of experimental measurements[11,12] reporting nonbulk behavior, but also by the existence of accurate many-body potentials appropriate to model them.[26] The present work builds on earlier efforts from the computational modeling community which already discussed the specific character of vibrations in nanoparticles,[6,7,24,27–30] and the validity of the Debye model to describe in particular the low temperature heat capacity.[24,25] Here we extend the scope to the mean square atomic displacement as an alternative property from which Θ_D can be inferred (instead of deriving this property from the vibrational properties themselves), cover an extended size range, and provide a critical discussion of the relation between the Debye and melting temperatures, in the case of ideal iron nanoparticles.

Our results suggest that for these systems the Debye model can be used to describe quantitatively the heat capacity of finite nanoparticles over a broad size range, but does not perform as strongly to model the mean square atomic displacement. Despite such limitations, the Debye temperatures inferred from either quantity are found to scale linearly with inverse particle radius, as expected from classical thermodynamical theories. However, comparison with the melting temperature obtained independently for the same nanoparticles and the same underlying model shows that the Debye and melting temperature do not vary in the expected square ratio, but a cubic exponent is numerically predicted instead.

The article is organized as follows. In the next section we briefly recall the main features of the Debye model for lattice vibrations of a solid, and how the heat capacity and mean square atomic displacement are computed for nanoparticles described atomistically. Sec. III presents and discusses the results obtained for and from the heat capacities, while Sec. IV focuses on the mean square atomic displacement. The size variations of the Debye temperature and their comparison with available experimental results are the subject of V, where we also critically discuss the relation with the melting temperature. Some concluding remarks are finally given in Sec. VI.

II. METHODS

We consider iron nanoparticles taken from the bcc arrangement and truncated at surfaces according to the ideal Wulff construction, yielding sizes of $N = 51$, 169, 363, 1013, 1603, 2381, 4279, 7495, 11 337, and 14 039 atoms. The interaction model is taken from the work by Mendelev and coworkers,[26] in which the energetic, thermal, and vibrational properties of iron in the bcc and fcc solid phases but also in the liquid state are reproduced fairly well. The choice of a model that performs well not only for vibrations but also for phase transitions turns out to be rather important for the present work, in which the Debye temperature and the melting temperature will tentatively be connected to one another (vide infra). While the Wulff construction is expected to produce very low energy structures for medium to large nanoparticles, even lower minima might exist in the very low size limit due to strongly nonmonotonic finite size effects. While this global optimization is interesting in itself, we have not attempted to solve it here, focusing instead on finite size effects in the scaling regime.[23]

The Debye model assumes that the vibrational density of states (VDOS) $g_D(\omega)$ of a solid scales with frequency ω as $g_D(\omega) \propto \omega^2 H(\omega_{max}-\omega)$, where H is the Heaviside step function and ω_{max} a maximum frequency that defines the Debye temperature Θ_D through $\hbar\omega_{max} = k_B\Theta_D$, k_B being the Boltzmann constant. The Debye model predicts a lattice contribution to the heat capacity that reads

$$C_v^{Debye}(T) = 9Nk_B\left(\frac{T}{\Theta_D}\right)^3 \int_0^{\Theta_D/T} \frac{x^4 e^x}{(e^x-1)^2} dx. \quad (1)$$

In bulk solids, the mean square atomic displacement (MSD) σ^2 can also be connected to the Debye tempera-

ture through[10]

$$\sigma^2_{\mathrm{Debye}}(T) = \frac{9\hbar^2}{mk_{\mathrm{B}}\Theta_{\mathrm{D}}}\left[\frac{1}{4} + \left(\frac{T}{\Theta_{\mathrm{D}}}\right)^2 \int_0^{\Theta_{\mathrm{D}}/T} \frac{xe^x}{e^x-1}dx\right]. \quad (2)$$

where m is the atomic mass and $\hbar$ the reduced Planck constant, respectively.

In experiments on real systems, Debye temperatures are extracted from either of these quantities, assuming that the Debye quadratic model of vibrations can be used to describe either specific values of C_v or σ^2 at a prescribed measurement temperature, or their entire variations over a temperature range. Depending on the details of the fitting procedure, the value of Θ_{D} that results from this adjustment may thus carry a temperature dependence itself, or be more robust and characteristic of the system over a broader range of conditions. In the remainder of this article, we choose to define a system-specific but temperature-independent Debye temperature from the variations of C_v or σ^2 over an entire temperature range, and refer interested readers to the works by Garzón and coworkers[24] on the additional features introduced by considering the measurement temperature as an extra parameter in the case of sodium microclusters.

A similar procedure can be followed to define Debye temperatures for systems in which the VDOS does not strictly follow the Debye model of lattice vibrations, as is the case for finite nanoparticles. From the knowledge of the actual vibrational density $g(\omega)$, the canonical heat capacity and mean square atomic vibrations are defined respectively as

$$C_v(T) = \int \frac{\hbar\omega^2}{k_{\mathrm{B}}T^2} \frac{\exp(\hbar\omega/k_{\mathrm{B}}T)}{[\exp(\hbar\omega/k_{\mathrm{B}}T)-1]^2} g(\omega)d\omega \quad (3)$$

$$\sigma^2(T) = \frac{1}{2Nm}\int \frac{\hbar}{\omega\tanh\left(\hbar\omega/2k_{\mathrm{B}}T\right)} g(\omega)d\omega \quad (4)$$

Equations 1 and 2 are naturally recovered by inserting g_{D} in lieu of g in the above expressions.

In a first approach, the VDOS of nanoparticles can be obtained in the harmonic approximation that is expected to be valid at low temperatures:

$$g(\omega) = \sum_{i=1}^{3N-6} \delta(\omega-\omega_i), \quad (5)$$

where $\{\omega_i, i = 1\cdots 3N-6\}$ are the normal mode frequencies obtained after diagonalizing the dynamical matrix. However, such a diagonalization procedure is computationally costly as it scales with N^3, which its application to nanoparticles of a few thousands of atoms only. Alternatively, the VDOS can be numerically obtained by Fourier transforming the time autocorrelation function of the atomic velocities, $g(\omega) \propto \mathcal{F}[\gamma(t)]$ where

$$\gamma(t) = \frac{\langle\sum_i \vec{v}_i(t)\cdot\vec{v}_i(0)\rangle}{\langle\sum_i \|\vec{v}_i(0)\|^2\rangle} \quad (6)$$

which can be straightforwardly obtained from time series accumulated in molecular dynamics simulations. This procedure has the advantage of incorporating finite temperature anharmonicities, and scales only as N^2 with the number of atoms through the gradient evaluation needed during the MD propagation. Here we initiate 20 independent MD trajectories from the global minimum structure and let them evolve at constant total energy (microcanonical ensemble) chosen to yield a kinetic temperature of about 300 K. The individual trajectories used to generate the VDOS were each propagated for 100 ps, after 20 ps equilibration, and employed a time step of 1 fs.

Classical and path-integral molecular dynamics (PIMD) simulations at constant temperature were also performed to calculate the mean square atomic displacement σ^2. Nosé-Hoover thermostats were applied to the atoms or all of the P replicas in the PIMD description. A Trotter discretization number of $P = 64$ was used for temperatures in the range of 1–100 K, with a time step of 0.1 fs and a total integration time of 100 ps, for nanoparticles containing up to 1013 atoms. Classical trajectories were also conducted for sizes up to 14 039 atoms, over times of 100 ps and a time step of 1 fs, but over the extended temperature range of 10–500 K. Finally, additional trajectories were performed for body-centered cubic (bcc) samples under periodic boundary conditions in the minimum image convention, for system sizes of 2000 and 8192 atoms, to assess the importance of surface effects in the limit of large sizes.

III. DEBYE TEMPERATURE FROM HEAT CAPACITIES

Fig. 1 shows the vibrational densities of states obtained for three iron nanoparticles in the size range of 363–2183 atoms after Fourier transforming the time autocorrelation function of atomic velocities at 300 K, as well as the corresponding harmonic densities that are valid in the zero temperature limit. These densities exhibit a progressive and rather monotonic evolution as the nanoparticle size increases, in particular with the main peak near 260 cm^{-1} that becomes increasingly high and narrow. The acoustic gap, which is defined as the lowest excitable frequency, decreases in the harmonic limit as the nanoparticle becomes larger, but this feature does not appear as markedly for the anharmonic VDOS owing to its continuous nature. We show in Fig. 2 the variations of the canonical heat capacities $C_v(T)$ obtained for the two smaller nanoparticles but also for the periodic 2000-atom bcc system using again both the corresponding harmonic and anharmonic (300 K) densities of states. These quantities exhibit smoothly increasing variations, the Dulong-Petit classical limit $C_v(T\to\infty) \simeq 3k_{\mathrm{B}}$/atom being almost reached at 500 K. Anharmonicities tend to decrease the heat capacities by a minor amount, but this effect is noticeable only in the strongly quantum regime

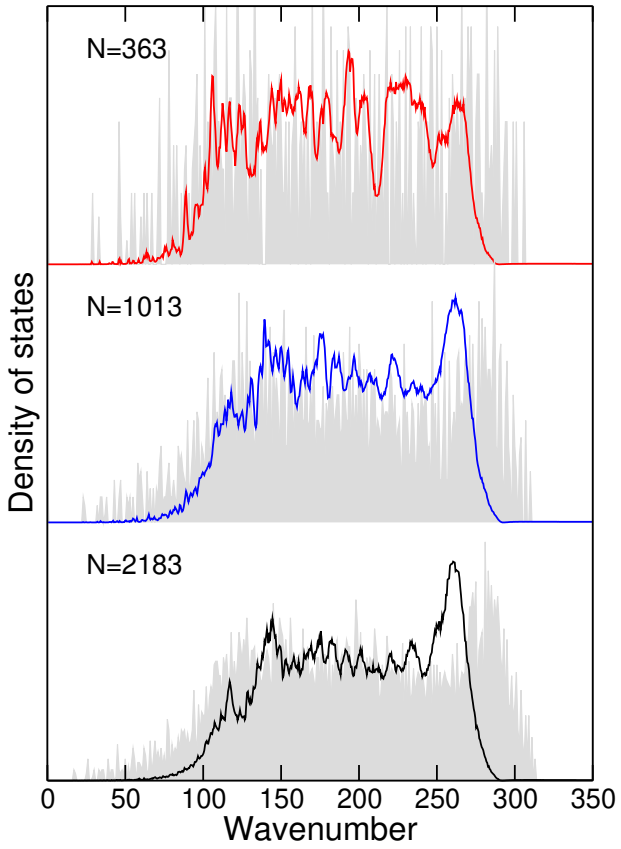

FIG. 1. Vibrational densities of states obtained at 300 K for Fe_N nanoparticles with 363, 1013, and 2183 atoms. The harmonic densities of states are superimposed in the background as grey lines. No broadening of any kind was imposed to the results.

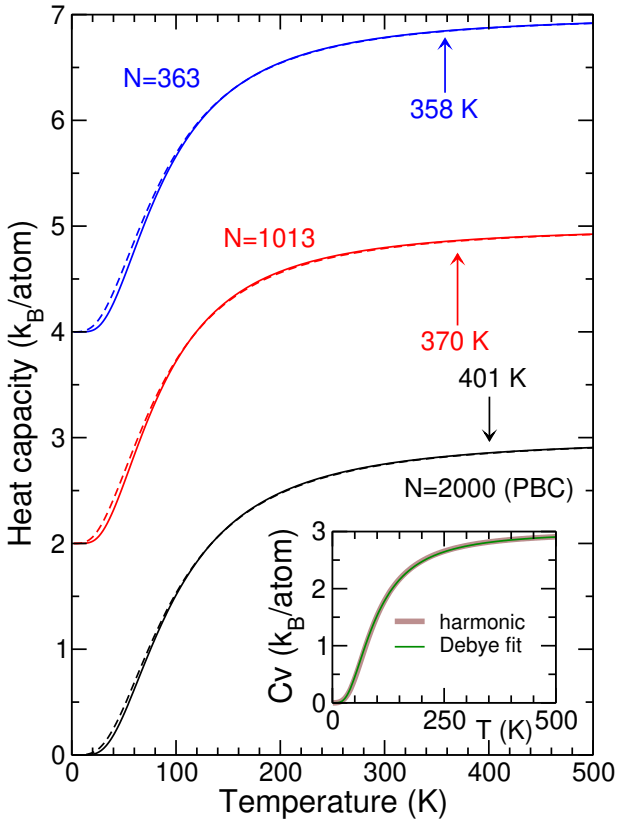

FIG. 2. Lattice canonical heat capacities of Fe_N nanoparticles with $N = 363$ and $N = 1013$, and for a periodic 2000-atom bcc sample, obtained from the anharmonic vibrational density of states at 300 K (solid lines) and in the harmonic limit (dashed lines). The curves for the two nanoparticles were shifted for clarity, and the vertical arrows mark the value of the Debye temperatures inferred from fitting the anharmonic heat capacities to a Debye model. The inset shows the quality of such a Debye fit against the harmonic prediction for the periodic 2000-atom sample.

$T < 100$ K.

Although the vibrational densities of states clearly deviate from the assumptions of the Debye model, Eq. (1) provides a quantitative description of the heat capacity obtained from applying Eq. (3) to the VDOS calculated for each specific system, provided that Θ_D is numerically adjusted to each specific system. An example of such a quantitative modeling is shown as an inset in Fig. 2 for the periodic system in the harmonic limit.

The Debye temperatures of the 1013-atom nanoparticle obtained by fitting the entire reference heat capacity curves of Fig. 2 onto the Debye form of Eq. (1) are found to be 372 K and 370 K for the harmonic and anharmonic models of the VDOS, respectively, or about 100 K lower than the low-temperature limit bulk Debye temperature of α iron,[31] and close to the room temperature Θ_D of the same material (373 K, Ref. 32). For the smaller nanoparticle these values drop to 364 K and 358 K, respectively, while for the 2000-atom periodic sample we find 397 K and 401 K, respectively, in much closer agreement with the experimental temperature for bulk alpha iron. From simulations performed for the 8192 bcc sample, we find $\Theta_D = 403$ K in the 300 K anharmonic model, indicating that residual finite size effects due to the periodic cell remain very limited.

At 300 K, anharmonicities amount to only about 1% deviation in the numerically estimated Debye temperature, alhough it is intersting to note that in the case of the periodic system the anharmonic Θ_D is higher than the harmonic value, the opposite being found for the nanoparticles.

IV. DEBYE TEMPERATURE FROM MEAN SQUARE ATOMIC DISPLACEMENT

Another way of accessing the Debye temperature is based on the mean square atomic displacement, which can be numerically determined in the classical limit by thermostatted MD simulations, and more rigorously by incorporating nuclear quantum effects using path-integral (PI) MD simulations. It can also be related to

the VDOS through Eq. (4). Fig. 3(a,b) show the variations of $\sigma^2(T)$ obtained for the same 363- and 1013-atom iron nanoparticles as a function of increasing temperature, using the classical and quantum harmonic approximations as well as the anharmonic MD and PIMD data. We also show in Fig. 3(c) the corresponding variations for the periodic 2000-atom bcc sample, for which the PIMD approach was found to be unpractical.

For nanoparticles, a simple expression for $\sigma^2(T)$ is found to accurately interpolate between the low-temperature, quantum but nearly harmonic behavior and the high-temperature, anharmonic but nearly classical behavior:

$$\sigma^2(T) \simeq \frac{3N-6}{2mN} \frac{\hbar}{\omega_{\rm eff} \tanh\left(\hbar\omega_{\rm eff}/2k_{\rm B}T\right)}, \qquad (7)$$

in which we have introduced a single parameter $\omega_{\rm eff}$ as size-dependent effective frequency. This expression for $\sigma^2(T)$ will be refered to as the anharmonic model for the MSD.

The phenomenological quantum anharmonic model can also be applied to the bulk sample, by extrapolating the effective frequency $\omega_{\rm eff}$ obtained for increasing large nanoparticles. The inset of Fig. 3(b) shows the variations of $\omega_{\rm eff}$ with $N^{-1/3}$, which is proportional to the inverse particle radius. In a very good approximation, these variations are essentially linear and can be described as

$$\omega_{\rm eff}(N) = 176.8 - 155.0N^{-1/3} + \mathcal{O}(N^{-2/3}), \qquad (8)$$

where the frequency is expressed in $\rm cm^{-1}$. This simple function provides a convenient way of extrapolating the double dependence of the MSD on size and temperature, from which a Debye temperature can be estimated as a continuous function of size. Applying the model in the bulk limit $N \to \infty$, the low-temperature quantum harmonic limit and the high temperature classical anharmonic limit are both correctly recovered for the periodic 2000-atom bcc sample, as can be seen in Fig. 3(c).

Comparing the results obtained for the three systems shown in Fig. 3, the most striking difference is the decreasingly lower rate of variations in the MSD as a function of increasing temperature, as the system size itself increases. This effect is a clear manifestation of the larger proportion of surface atoms in the smaller nanoparticles, and their greater ability to move relative to the more constrained and more coordinated bulk atoms.

Similarly as with the heat capacity, Debye temperatures can now be extracted from the temperature variations of the MSD by fitting them onto the one-parameter function of Eq. (2). For the 1013-atom nanoparticle, the resulting values for $\Theta_{\rm D}$ are found to be 210 K and 245 K for the harmonic and anharmonic descriptions of atomic vibrations, respectively, now significantly lower than the experimental bulk values but also lower than the values obtained from fitting the specific heat. In the smaller 363-atom system, these temperatures drop to 204 K and 236 K, respectively. Conversely but unsurprisingly, for the periodic system we find higher values of 259 K and 272 K, respectively.

It is worth noting in Fig. 3 that the Debye model does not perform very well in reproducing the actual variations of $\sigma^2(T)$, particularly at low temperature where the true MSD is significantly overestimated, even though the differences are not as marked for the periodic sample. Such discrepancies are thus a typical manifestation of the errors introduced when applying bulk concepts to small size objects characterized by highly discretized state densities. In any case, the lower Debye temperature obtained from fitting the MSD, relative to the value obtained from fitting the heat capacity, is consistent with the two experimental values known for bulk α iron and the different methodologies they originate from.[31,32]

V. FINITE SIZE EFFECTS AND SCALING LAWS

Anharmonic values of $\Theta_{\rm D}$ based on fitting the heat capacity obtained from the continuous VDOS $g(\omega)$, as well as the two values from either C_v or σ^2 but in the harmonic approximations, are represented in Fig. 4 as a function of $N^{-1/3}$. These four ways of determining $\Theta_{\rm D}$ lead to essentially linear variations with increasing $N^{-1/3}$, the negative slope being always indicative that the Debye temperature *increases* with increasing particle size. The values extrapolated at the bulk limit $N^{-1/3} \to 0$ are 410 K and 401 K from the heat capacity in the anharmonic and harmonic descriptions, respectively. These temperatures are close to those obtained using the same computational procedure but on the 2000-atom periodic samples, which confirms that the Wulff nanoparticles chosen here correctly extrapolate to the bulk material with the same lattice symmetry.

Using now the mean square atomic displacement to define $\Theta_{\rm D}$, extrapolating the nanoparticle data to the bulk limit $N^{-1/3} \to 0$ yields values of 272 K and 228 K in the anharmonic and harmonic descriptions, respectively, the former being consistent, by construction, with the calculations performed for the periodic sample. However, in the harmonic limit the extrapolated value is lower by about 30 K with respect to the Debye temperature fitted to reproduce the MSD of the periodic sample assuming harmonic oscillators, which is consistent with the lesser ability of the Debye model to account for the simulation results for the MSD observable.

Two sets of experimental measurements of Debye temperatures are available for iron nanoparticles. Herr and coworkers[11] used Mössbauer spectroscopy to determine the mean square atomic displacement in nanocrystalline iron, for particle sizes of about 6 nm diameter, for which they measured $\Theta_{\rm D} \approx 345$ K. Cuenya *et al.*[12] used near-resonant inelastic x-ray scattering (NRIXS) to evaluate various thermodynamical and structural quantities, and also extracted $\Theta_{\rm D}$ from the temperature variations of the

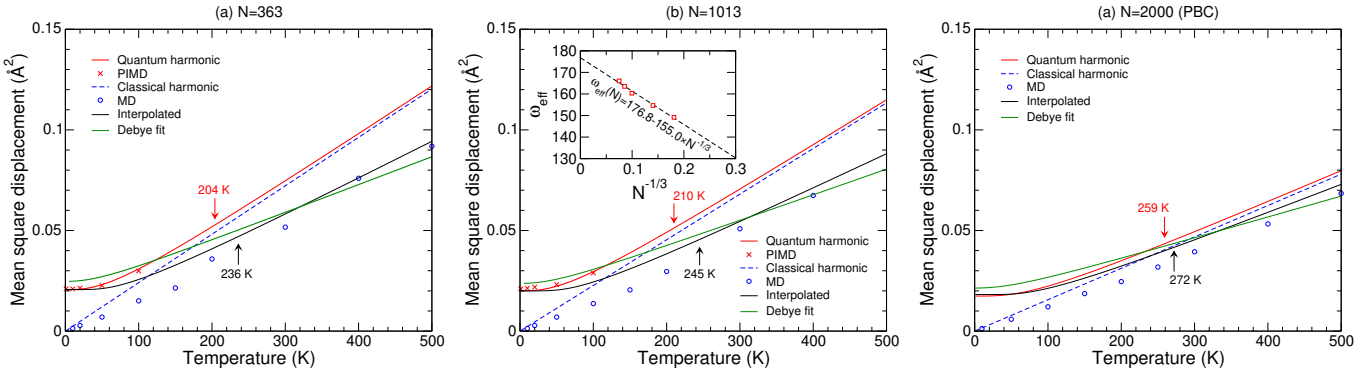

FIG. 3. Mean square atomic displacement obtained for Fe_N nanoparticles with (a) $N = 363$; (b) $N = 1013$; (c) a 2000-atom bcc sample, from the classical (dashed blue line) and quantum (solid red line) harmonic models, from classical MD (blue circles) and path-integral MD (red crosses, nanoparticles only). The black and green solid lines show the predictions of the interpolation model and the corresponding best Debye fit, respectively, with vertical arrows pointing at the equivalent Debye temperature obtained in the harmonic and anharmonic descriptions. The inset in panel (b) shows the variations of the effective frequency in the interpolation model with increasing inverse particle radius $N^{-1/3}$.

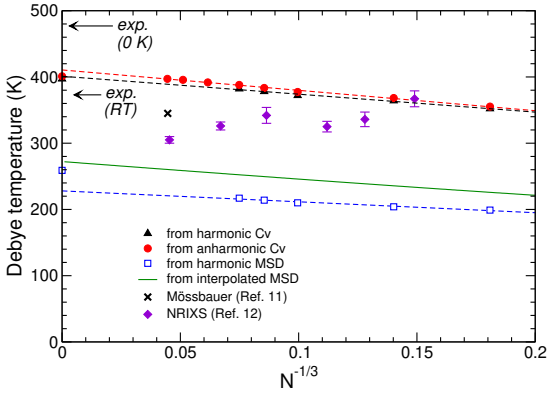

FIG. 4. Debye temperatures of Fe_N nanoparticles as a function of inverse particle radius $N^{-1/3}$, obtained from fitting the heat capacity or the mean square atomic displacement using harmonic or anharmonic data, and from available experimental measurements. The experimental Debye temperatures for bulk α iron at 0 K and room temperature are also highlighted by black left arrows, and the simulation results obtained for the periodic 2000-atom bcc sample are also indicated.

MSD for nanoparticles ranging from 2 to 6 nm diameter. As seen from Fig. 4, the range of these experimental Debye temperatures is consistent with our theoretically calculated values, and the results for the 2 nm nanoparticles are even in quantitative agreement, provided the heat capacity is used to define Θ_D. However, the decreasing trend found by Cuenya and coworkers for $\Theta_D(N)$ is not reproduced at all here. It is important to realize that, in both sets of experiments, the nanoparticles were not strictly isolated, but inserted in condensed environments or deposited. Following Cuenya and coworkers,[12,22] we attribute the surprising behavior found in the NRIXS experiments to either the consequence of the environment of the nanoparticles (titanium matrix) or to possible measurements artifacts.[22]

Finally, our calculated data can be used to challenge the macroscopic approaches to the Debye temperature, which based on the Lindemann theory of melting predict that Θ_D should scale linearly[15] with the square root of the melting temperature T_m. To assess this phenomenological theory, we have calculated independently from the Debye temperature the melting points of iron nanoparticles containing up to about 28 000 atoms, using classical molecular dynamics. Here a slow heating protocol was applied, the temperature being maintained again through the Nosé-Hoover method, and increased continuously at a rate of 0.3 K/ps. The excess internal energy $U(T)$ measured relative to the global energy minimum was estimated from the average potential energy, added to the average kinetic energy of $(3N - 6)k_BT/2$. The melting temperature is identified as the value where the melting curve $U(T)$ exhibits a strong increase.

Such simulations were carried out for nanoparticles sizes covering the rather broade size range extending up to 27937 atoms, always assuming a perfect Wulff shape as the solid form at zero temperature. The variations of the internal energy with increasing temperature are shown in Fig. 5(b) for the various nanoparticles. For all sizes N, a melting temperature $T_m(N)$ can be estimated as the value where the internal energy exhibits a strong jump that marks the latent heat of melting. For the present nanoparticles we generally find that the melting temperature increases monotonically with increasing nanoparticle size, this being the expected result in the scaling regime.[33]

For a given nanoparticle, the melting point $T_m(N)$ was defined from the temperature variations of the internal energy $U(T)$ as the value at which $U(T)$ shows a marked increase, indicative of the latent heat of melting. Typical internal energy curves are shown in Fig. 5 for three selected nanoparticle sizes.

The melting temperature thus obtained exhibits linear variations with inverse particle radius $N^{-1/3}$, as shown

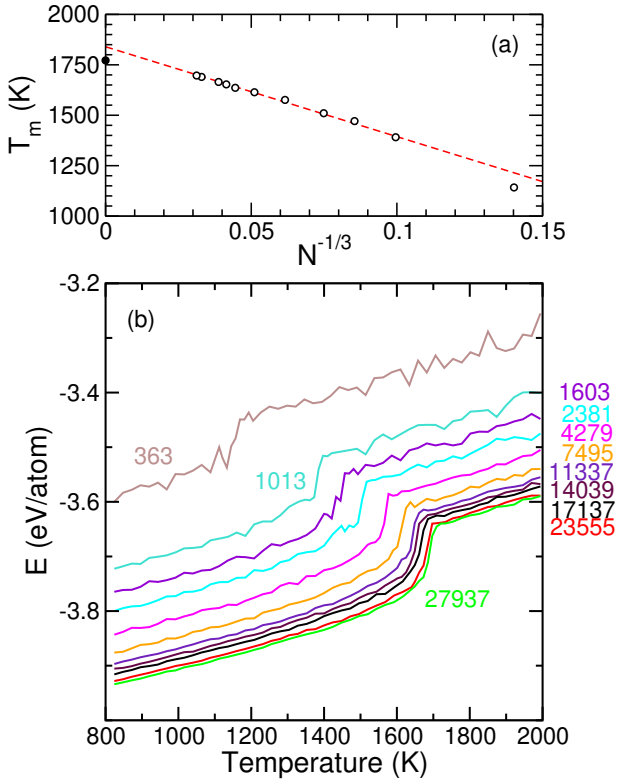

FIG. 5. Melting behavior of Fe_N nanoparticles from molecular dynamics simulations. (a) Melting temperature as a function of $N^{-1/3}$, with the bulk value taken from Ref. 26; (b) Internal energy as a function of temperature for particles containing $N = 363$–27937 atoms.

in Fig. 5(a). Extrapolation to the bulk limit $N^{-1/3} \to 0$ gives a bulk melting temperature of 1840 K, in fairly good agreement with the experimental value of 1811 K for bulk α iron, but also in satisfactory agreement with the simulated values reported by Shu and coworkers.[34] Here we note that the value originally reported by Mendelev and coworkers[26] who developed the present potential (1758 K) is substantially lower that those obtained here and more recently by this other group. This might be attributed to the different computational protocol employed by Mendelev *et al.* and possibly less converged simulations.

From the computational results, the size variations of the melting temperature of iron nanoparticles are quantitatively described at lowest correcting order as

$$T_m(N) \simeq T_m^\infty (1 - aN^{-1/3}), \tag{9}$$

where $a > 0$ is a parameter. Likewise, a linear scaling relation with inverse particle radius applies to the Debye temperature Θ_D, which we write as

$$\Theta_D(N) \simeq \Theta_D^\infty (1 - bN^{-1/3}), \tag{10}$$

$b > 0$ being another parameter which also depends on the choice of the observable (heat capacity of mean square atomic displacement) used to define the Debye temperature.

The scaling of Θ_D with the square root of T_m would imply that $b = a/2$ at leading order. Here we have determined the size variations of the melting point independently from those of the Debye temperature, and extrapolated them to the respective bulk limits, fitting the corresponding data to evaluate the parameters a and b.

The scaled variations of the melting are represented in Fig. 6 as a function of $N^{-1/3}$, together with those obtained for the Debye temperatures inferred from fitting the heat capacity or the mean square atomic displacement, both in the anharmonic models. The slopes are

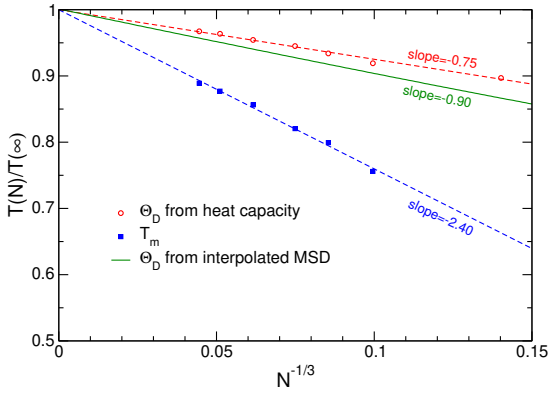

FIG. 6. Variations of the Debye and melting temperatures of iron nanoparticles as a function of inverse particle radius $N^{-1/3}$, scaled by their bulk limiting value. For the Debye temperature, the two sets of data obtained from the anharmonic heat capacity or the mean square atomic displacement are shown.

found to be $b = 0.75$–0.9 for Θ_D and $a = 2.4$ for T_m, or a ratio a/b much closer to 3 than to the value of 2 expected from the Lindemann argument. The present results are thus consistent with a scaling relation between the Debye and melting temperatures but of the type

$$T_m(N) \propto \Theta_D^3(N), \tag{11}$$

and this result appears robust against the choice of the observable used to define the Debye temperature.

VI. DISCUSSION AND CONCLUSIONS

Our predictions for the Debye temperature of iron nanoparticles are consistent with the general depression in the softening of vibrational modes due to surface atoms, and with variations that are linear with inverse particle radius for a 3D nanosystem. They also confirm that these variations can be described as scaling laws, but with coefficients that are about 1/3 of those in the melting temperature. However, the differences known already in the bulk system regarding the two alternative ways of defining Θ_D based on the low temperature heat

capacity or on the finite temperature mean square atomic displacement convey at the nanoscale with similar differences (exceeding 100 K, or 30%).

Obviously, the present calculations are prone to several sources of error, starting with the underlying atomistic model to describe bcc iron,[26] which is of high quality but always perfectible. Unfortunately, extracting the vibrational properties of nanoparticles containing 10^3–10^4 atoms using methods that explicitly account for electronic structure seems unfeasible with the presently available methods. Another approximation made lies in the use of classical MD to extract the anharmonic vibrational density of states, used in a subsequent step to calculate the lattice contribution to the (quantum) heat capacity. Despite being rather conventional, this approach could be improved by incorporating nuclear quantum effects already from the start, possibly through methods based on path-integral molecular dynamics such as ring-polymer MD. However, such approaches are also computationally costly, and suffer from known resonance problems when applied to vibrational spectroscopy.[35] Incidentally, the melting temperatures were also evaluated from classical MD, but here the neglect of nuclear quantum effects is probably well justified.

Notwithstanding such possible minor issues, our computational results remain robust and confirm the difficulties associated with a unique definition for the Debye temperature of nanoscale systems, based on concepts that are intrinsically macroscopic. It would next be of particular interest to extend the presently developed methodologies to other types of nanoscale systems, under isolated conditions but also, more importantly, deposited on substrates or embedded in matrices.

[1] A. Ahmed, M. Pelton, and J. R. Guest, ACS Nano **11**, 9360 (2017).
[2] M. Chen, F. Cai, C. Wang, Z. Wang, L. Meng, F. Li, P. Zhang, X. Liu, and H. Zheng, Adv. Sci. **4**, 1600447 (2017).
[3] W. Heni, L. Vonna, and H. Haidara, Nano Lett. **15**, 442 (2015).
[4] A. Alkurdi, J. Lombard, F. Detcheverry, and S. Merabia, Phys. Rev. Appl. **13**, 034036 (2020).
[5] A. Balerna, E. Bernieri, P. Picozzi, A. Reale, S. Santucci, E. Burattini, and S. Mobilio, Phys. Rev. B **31**, 5058 (1985).
[6] M. Bayle, N. Combe, N. M. Sangeetha, G. Viau, and R. Carles, Nanoscale **6**, 9157 (2014).
[7] R. Carles, P. Benzo, B. Pécassou, and C. Bonafos, Sci. Rep. **6**, 39164 (2016).
[8] S. I. Sanchez, L. D. Menard, A. Bram, J. H. Kang, M. W. Small, R. G. Nuzzo, and A. I. Frenkel, J. Am. Chem. Soc. **131**, 7040 (2009).
[9] B. Roldan Cuenya, M. Alcántara Ortigoza, L. K. Ono, F. Behafarid, S. Mostafa, J. K. Croy, K. Paredis, G. Shafai, T. S. Rahman, L. Li, Z. Zhang, and J. C. Yang, Phys. Rev. B **84**, 245438 (2011).
[10] M. Hou, M. El Azzaoui, H. Pattyn, J. Verheyden, G. Koops, and G. Zhang, Phys. Rev. B **62**, 5117 (2000).
[11] U. Herr, J. Jing, B. Birringer, U. Gonser, H. Gleiter *et al.*, Appl. Phys. Lett. **50**, 472 (1987).
[12] B. Roldan Cuenya, L. K. Ono, J. R. Croy, K. Paredis, A. Kara, H. Heinrich, J. Zhao, E. E. Alp, A. T. DelaRiva, A. Datye, E. A. Stach, and W. Keune, Phys. Rev. B **86**, 165406 (2012).
[13] U. Herr, M. Geigl, and K. Samwer, Philos. Mag. A **77**, 641 (1998).
[14] C. C. Yang, M. X. Xiao, W. Li, and Q. Jiang, Solid State Commun. **139**, 148 (2006).
[15] C. C. Yang, and S. Li, Phys. Status Solidi B **248**, 1375 (2011).
[16] K. Sadayiandi, Mater. Chem. Phys. **115**, 703 (2009).
[17] G. Ouyang, Z. M. Zhu, W. G. Zhu, and C. Q. Sun, J. Phys. Chem. C **114**, 1805 (2010).
[18] F. Calvo, J. Phys. Chem. C **115**, 17730 (2011).
[19] H. E. Sauceda, D. Mongin, P. Maioli, A. Crut, M. Pellarin, N. Del Fatti, F. Vallée, and I. L. Garzón, J. Phys. Chem. C **116**, 25147 (2012).
[20] W.-H. Li, S. Y. Wu, C. C. Yang, S. K. Lai, K. C. Lee, H. L. Huang, and H. D. Yang, Phys. Rev. Lett. **89**, 135504 (2002).
[21] B. Roldan Cuenya, A. I. Frenkel, S. Mostafa, F. Behafarid, J. R. Croy, L. K. Ono, and Q. Wang, Phys. Rev. B **82**, 155450 (2010).
[22] J. Timoshenko, M. Ahmadi, and B. Roldan Cuenya, J. Phys. Chem. C **123**, 20594 (2019).
[23] J. Jortner, Z. Phys. D: At. Mol. Clusters **24**, 247 (1992).
[24] H. E. Sauceda, F. Salazar, L. A. Pérez, and I. L. Garzón, J. Phys. Chem. C **117**, 25160 (2013).
[25] G. Shafai, M. Alcántara Ortigoza and T. S. Rahman, J. Phys.: Cond. Matt. **24**, 104026 (2012).
[26] M. I. Mendelev, S. Han, D. J. Srolovitz, G. J. Ackland, D. Y. Sun, and M. Asta, Philos. Mag. **83**, 3977 (2003).
[27] R. Meyer, L. J. Lewis, S. Prakash, and P. Entel, Phys. Rev. B **68**, 104303 (2003).
[28] D. Şopu, J. Kotakoski, and K. Albe, Phys. Rev. B **83**, 245416 (2011).
[29] A. S. Maldonado, G. F. Cabeza, and S. B. Ramos, J. Phys. Chem. Solids **131**, 131 (2019).
[30] A. Kara and T. S. Rahman, Phys. Rev. Lett. **81**, 1453 (1998).
[31] A. Tari, The Specific Heat of Matter at Low temperatures (Imperial College Press, London, 2003).
[32] C. Y. Ho, R. W. Powell, and P. E. Liley, J. Phys. Chem. Ref. Data **3**, 1 (1974).
[33] Ph. Buffat and J.-P. Borel, Phys. Rev. A **13**, 2287 (1976).
[34] Q. Shu, Y. Yang, Y.-T. Zhai, D. Y. Sun, H. J. Xiang, and X. G. Gong, Nanoscale **4**, 6307 (2012).
[35] A. Witt, S. D. Ivanov, M. Shiga, H. Forbert, and D. Marx, J. Chem. Phys. **130**, 194510 (2009).